Fully strange tetraquark states via QCD sum rules*

Bing-Dong Wan (万秉东)[1,2†] Ji-Chong Yang (杨冀翀)[1,2‡]

[1]Department of Physics, Liaoning Normal University, Dalian 116029, China
[2]Center for Theoretical and Experimental High Energy Physics, Liaoning Normal University, Dalian 116029, China

Abstract: In this paper, we systematically explore the mass spectrum of fully strange tetraquark candidates within the framework of QCD sum rules, focusing on states with quantum numbers $J^{PC} = 0^{++}$, 0^{-+}, 0^{--}, 1^{--}, 1^{+-}, and 1^{++}. The analysis reveals the existence of fully strange tetraquark states with masses ranging from approximately 2.07 to 3.12 GeV. These predictions are compared with existing experimental observations of potential fully strange tetraquark resonances, notably the $X(2300)$ recently reported by the BESIII Collaboration, which may be interpreted as a fully strange tetraquark state. Furthermore, the possible decay modes of these fully strange tetraquark states are analyzed, providing guidance for their identification in current and future high-energy experiments, such as BESIII, Belle II, and LHCb.

Keywords: exotic hadron, QCD sum rules, mass

DOI: 10.1088/1674-1137/ae2fc8 **CSTR:** 32044.14.ChinesePhysicsC.50043104

I. INTRODUCTION

The study of novel hadronic states—such as multiquarks, hybrids, and glueballs—has gained significant attention in recent years as experimental and theoretical advances continue to challenge the conventional quark model [1, 2]. Since the discovery of the $X(3872)$ state [3], more than thirty similar novel states or candidates have been reported in various experiments. This growing list of observations strongly suggests that many more new hadronic states are likely to be discovered in the near future, marking a renaissance in hadron spectroscopy. Unraveling the internal structure and underlying dynamics of these newly observed states constitutes one of the most compelling and significant challenges in contemporary hadron physics.

In the light hadron sector, the identification of novel hadronic states remains a significant challenge, primarily due to the small mass splittings between states and the resulting strong mixing among them. This often obscures the distinction between novel and conventional configurations in experimental analyses, except that the novel hadronic states possessing exotic quantum numbers, which are forbidden in the conventional quark model, offer cleaner signatures for identifying nontraditional structures. However, with the rapid accumulation of high-precision experimental data in the charm quark sector, the BESIII experiment is now well-positioned to conduct a systematic investigation of hadronic phenomena in this energy region—including, crucially, the search for and study of light novel hadrons [4−13].

Among the various novel hadron candidates, fully strange tetraquark states—composed entirely of two strange quarks and two strange antiquarks ($ss\bar{s}\bar{s}$)—constitute a particularly intriguing and theoretically clean subclass. Owing to their flavor purity, these states are free from mixing with light (u, d) or heavy (c, b) quark components, offering a uniquely controlled environment for investigating fundamental aspects of QCD, including quark confinement, color dynamics, and gluon-mediated interactions. Their distinct quark content also enhances their stability against decay into lighter mesons via quark flavor rearrangement. Notably, fully strange tetraquarks can accommodate exotic quantum numbers—such as $J^{PC} = 0^{--}$—which are strictly forbidden in conventional quark–antiquark meson configurations. The observation of such states would thus serve as a clear indication of multiquark dynamics beyond the conventional hadron classification scheme.

Recently, the BESIII Collaboration reported the ob-

Received 20 October 2025; Accepted 22 December 2025; Accepted manuscript online 23 December 2025

* Supported in part by the National Natural Science Foundation of China (12575106, 12147214) and Specific Fund of Fundamental Scientific Research Operating Expenses for Undergraduate Universities in Liaoning Province (LJ212410165019)

† E-mail: wanbd@lnnu.edu.cn

‡ E-mail: yangjichong@lnnu.edu.cn

servation of a resonant structure, denoted as $X(2300)$, in a partial wave analysis of the process $\psi(3686) \to \phi\eta\eta'$ [14]. The structure appears prominently in the $\phi\eta$ and $\phi\eta'$ invariant mass spectra, with statistical significances of $9.6\,\sigma$ and $5.6\,\sigma$, respectively, and the measured decay width of the state is approximately 89 MeV. The measured mass of $X(2300)$ exhibits a notable discrepancy with the theoretical predictions for conventional strangeonium states, as reported in Refs. [15−21]. By contrast, the mass of the fully strange tetraquark state with quantum numbers $J^{PC} = 1^{+-}$, as calculated in Ref. [22], shows good agreement with the observed mass of $X(2300)$, suggesting a possible tetraquark interpretation. For further studies on fully-strange tetraquarks, the reader is referred to Refs. [23−29].

Motivated by the observation of the $X(2300)$ resonance, fully strange tetraquark states have attracted renewed attention, especially through the lens of QCD sum rule analyses [30], which provide a nonperturbative framework for exploring their possible structure and mass spectrum. QCD sum rules (QCDSR) constitute a QCD-based theoretical framework that systematically incorporates nonperturbative effects. This approach has been successfully applied to a wide range of problems in hadron spectroscopy, providing valuable insights into the structure and properties of conventional and novel hadrons [31−71]. The initial step in formulating QCD sum rules involves constructing appropriate interpolating currents that correspond to the hadrons under investigation. These currents encode essential information about the hadrons, such as their quantum numbers and internal structural components. Based on these interpolating currents, the two-point correlation function is defined, which admits two distinct representations: the operator product expansion (OPE) side and phenomenological side. By matching these two representations through a dispersion relation and applying quark-hadron duality, the QCD sum rules are established. This framework then enables the extraction of hadronic properties, such as the mass spectrum, from the underlying QCD dynamics.

In this work, the masses of the fully strange tetraquark states in molecular configurations with $J^{PC} = 0^{++}$, 0^{-+}, 0^{--}, 1^{--}, 1^{+-}, and 1^{++} are investigated within the framework of QCD sum rules. Because the 1^{-+} states were investigated in our previous work [31] and the 0^{+-} state does not admit a molecular configuration, these two states are excluded from the present analysis. The remainder of this paper is organized as follows. A concise overview of the QCD sum rules framework and the essential formulas employed in our calculations are presented in Sec. II. The numerical analysis and corresponding results are discussed in Sec. III. The possible tetraquark decay modes are given in Sec. IV. Finally, a brief summary and concluding remarks are provided in Sec. V.

II. FORMALISM

To evaluate the mass spectrum of fully strange tetraquark states within the QCD sum rule framework, the initial step is to construct suitable interpolating currents. The procedure for constructing these currents is as follows. First, all possible currents are listed, specifying their constituent quark content and corresponding Dirac gamma matrix structures.

In general, fully strange tetraquark states may possess a rich internal structure. Several types of interpolating currents have been widely discussed in the literature, including molecular (di-meson) currents, diquark–antidiquark currents, and color-adjoint currents. Each construction emphasizes a different possible organization of quarks and probes different components of the underlying QCD dynamics. Consequently, their predictions for the mass spectrum and decay properties may differ quantitatively.

In the present work, we choose to focus on the molecular-type currents of the form $[\bar{s}s][\bar{s}s]$, which are particularly suitable for describing possible meson–meson bound or resonant configurations in the fully strange sector. This choice is further motivated by the proximity of the expected masses to relevant two-meson thresholds and by the widespread use of such currents in previous QCD sum rule studies of exotic states. Therefore, we emphasize that the results presented in this paper are restricted to the molecular configuration and should be interpreted within this specific framework. A systematic and quantitative comparison among different current constructions, although highly interesting and important, is beyond the scope of the present work and is left for future investigations.

Subsequently, parity (P) and charge conjugation (C) transformations are applied to these currents to identify their transformation properties. By selecting the currents with the desired quantum numbers J^{PC} and eliminating redundant currents via Fierz rearrangements, a complete and non-redundant set of interpolating currents is obtained.

Via the aforementioned procedure, the interpolating currents for fully strange tetraquark states with $J^{PC} = 0^{++}$ in molecular configurations are constructed in the following forms:

$$j^{A}_{0^{++}}(x) = [\bar{s}_a(x)\gamma_5 s_a(x)][\bar{s}_b(x)\gamma_5 s_b(x)]\,, \tag{1}$$

$$j^{B}_{0^{++}}(x) = [\bar{s}_a(x) s_a(x)][\bar{s}_b(x) s_b(x)]\,, \tag{2}$$

$$j^{C}_{0^{++}}(x) = [\bar{s}_a(x)\gamma_\mu s_a(x)][\bar{s}_b(x)\gamma_\mu s_b(x)]\,, \tag{3}$$

$$j^{D}_{0^{++}}(x) = [\bar{s}_a(x)\gamma_\mu\gamma_5 s_a(x)][\bar{s}_b(x)\gamma_\mu\gamma_5 s_b(x)]\,, \tag{4}$$

$$j^{E}_{0^{++}}(x) = [\bar{s}_a(x)\sigma_{\mu\nu}s_a(x)][\bar{s}_b(x)\sigma_{\mu\nu}s_b(x)]\,, \tag{5}$$

where the subscripts a and b are color indices.

The interpolating currents for fully strange tetraquark states with $J^{PC} = 0^{-+}$ in molecular configurations are constructed in the following forms:

$$j^{A}_{0^{-+}}(x) = \mathrm{i}[\bar{s}_a(x)\gamma_5 s_a(x)][\bar{s}_b(x)s_b(x)]\,, \tag{6}$$

$$j^{B}_{0^{-+}}(x) = \mathrm{i}[\bar{s}_a(x)\sigma_{\mu\nu}s_a(x)][\bar{s}_b(x)\sigma_{\mu\nu}\gamma_5 s_b(x)]\,. \tag{7}$$

The interpolating currents for fully strange tetraquark states with $J^{PC} = 0^{--}$ in molecular configurations are constructed in the following forms:

$$j^{A}_{0^{--}}(x) = \mathrm{i}[\bar{s}_a(x)\gamma_\mu\gamma_5 s_a(x)][\bar{s}_b(x)\gamma_\mu s_b(x)]\,. \tag{8}$$

The interpolating currents for fully strange tetraquark states with $J^{PC} = 1^{--}$ in molecular configurations are constructed in the following forms:

$$j^{A,\mu}_{1^{--}}(x) = \mathrm{i}[\bar{s}_a(x)s_a(x)][\bar{s}_b(x)\gamma_\mu s_b(x)]\,, \tag{9}$$

$$j^{B,\mu}_{1^{--}}(x) = \mathrm{i}[\bar{s}_a(x)\sigma_{\mu\nu}\gamma_5 s_a(x)][\bar{s}_b(x)\gamma_\nu\gamma_5 s_b(x)]\,. \tag{10}$$

The interpolating currents for fully strange tetraquark states with $J^{PC} = 1^{+-}$ in molecular configurations are constructed in the following forms:

$$j^{A,\mu}_{1^{+-}}(x) = \mathrm{i}[\bar{s}_a(x)\gamma_5 s_a(x)][\bar{s}_b(x)\gamma_\mu s_b(x)]\,, \tag{11}$$

$$j^{B,\mu}_{1^{+-}}(x) = \mathrm{i}[\bar{s}_a(x)\sigma_{\mu\nu}s_a(x)][\bar{s}_b(x)\gamma_\nu\gamma_5 s_b(x)]\,. \tag{12}$$

The interpolating currents for fully strange tetraquark states with $J^{PC} = 1^{++}$ in molecular configurations are constructed in the following forms:

$$j^{A,\mu}_{1^{++}}(x) = \mathrm{i}[\bar{s}_a(x)s_a(x)][\bar{s}_b(x)\gamma_\mu\gamma_5 s_b(x)]\,, \tag{13}$$

$$j^{B,\mu}_{1^{++}}(x) = \mathrm{i}[\bar{s}_a(x)\sigma_{\mu\nu}\gamma_5 s_a(x)][\bar{s}_b(x)\gamma_\nu s_b(x)]\,. \tag{14}$$

With the currents in (1)−(14), the two-point correlation function can be readily established as follows:

$$\Pi^{k}_{J^{PC}}(q^2) = \mathrm{i}\int \mathrm{d}^4x\mathrm{e}^{\mathrm{i}q\cdot x}\langle 0|T\{j^{k}_{J^{PC}}(x),\ j^{k}_{J^{PC}}(0)^{\dagger}\}|0\rangle\,, \tag{15}$$

$$\Pi^{k}_{J^{PC},\,\mu\nu}(q^2) = \mathrm{i}\int \mathrm{d}^4x\mathrm{e}^{\mathrm{i}q\cdot x}\langle 0|T\{j^{k,\mu}_{J^{PC}}(x),\ j^{k,\nu}_{J^{PC}}(0)^{\dagger}\}|0\rangle\,. \tag{16}$$

Here, $\Pi(q^2)$ and $\Pi_{\mu\nu}(q^2)$ denote the correlation functions corresponding to states with spin $J = 0$ and 1, respectively; the index k runs from A to E for 0^{++} states, takes the value A for 0^{--} state, and runs from A to B in other cases; and $|0\rangle$ denotes the physical vacuum. The correlation function $\Pi_{\mu\nu}(q^2)$ corresponding to spin $J = 1$ states can be expressed in the following Lorentz-covariant form:

$$\Pi_{\mu\nu}(q^2) = -\Big(g_{\mu\nu} - \frac{q_\mu q_\nu}{q^2}\Big)\Pi_1(q^2) + \frac{q_\mu q_\nu}{q^2}\Pi_0(q^2)\,, \tag{17}$$

where the subscripts 1 and 0 denote the quantum numbers of the spin 1 and 0 mesons, respectively.

On the phenomenological side, the correlation function $\Pi(q^2)$ can be represented as a dispersion integral over the physical spectrum, with the ground-state tetraquark contribution explicitly isolated, *i.e.*,

$$\Pi^{\mathrm{phen},\,k}_{J^{PC}}(q^2) = \frac{(\lambda^{k}_{J^{PC}})^2}{(M^{k}_{J^{PC}})^2 - q^2} + \frac{1}{\pi}\int_{s_0}^{\infty}\mathrm{d}s\frac{\rho^{k}_{J^{PC}}(s)}{s - q^2}\,, \tag{18}$$

where M denotes the mass of the tetraquark state, λ is the coupling constant of the hadron, and $\rho(s)$ represents the spectral density, which encapsulates the contributions from higher excited states and the continuum above the threshold s_0.

In the OPE representation, the correlation function $\Pi(q^2)$ can be expressed through a dispersion relation as follows:

$$\Pi^{\mathrm{OPE},\,k}_{J^{PC}}(q^2) = \int_{s_{\min}}^{\infty}\mathrm{d}s\frac{\rho^{\mathrm{OPE},\,k}_{J^{PC}}(s)}{s - q^2} + \Pi^{\mathrm{sum},\,k}_{J^{PC}}(q^2)\,. \tag{19}$$

Here, $s_{\min}$ denotes the kinematic threshold, which typically corresponds to the squared sum of the current-quark masses of the hadron [32]. Π^{sum} represents the contributions to the correlation function that do not possess an imaginary part but yield nontrivial terms after the Borel transformation. The spectral density is given by $\rho^{\mathrm{OPE}}(s) = \mathrm{Im}[\Pi^{\mathrm{OPE}}(s)]/\pi$, and

$$\begin{aligned}\rho^{\mathrm{OPE}}(s) = {}& \rho^{\mathrm{pert}}(s) + \rho^{\langle\bar{s}s\rangle}(s) + \rho^{\langle G^2\rangle}(s) + \rho^{\langle\bar{s}Gs\rangle}(s) \\ & + \rho^{\langle\bar{s}s\rangle^2}(s) + \rho^{\langle G^2\rangle\langle\bar{s}s\rangle}(s) + \rho^{\langle\bar{s}s\rangle\langle\bar{s}Gs\rangle}(s)\,.\end{aligned} \tag{20}$$

To calculate the spectral density on the OPE side, as given in Eq. (20), the full light-quark propagator $S^{q}_{ij}(x)$ is utilized, namely

$$
\begin{aligned}
S^{q}_{ij}(x) = & \frac{\mathrm{i}\delta_{ij}\not{x}}{2\pi^2 x^4} - \frac{\delta_{ij} m_q}{4\pi^2 x^2} - \frac{\mathrm{i} t^a_{ij} G^a_{\alpha\beta}}{2^5 \pi^2 x^2}(\sigma^{\alpha\beta}\not{x} + \not{x}\sigma^{\alpha\beta}) \\
& - \frac{\delta_{ij}}{12}\langle\bar{q}q\rangle + \frac{\mathrm{i}\delta_{ij}\not{x}}{48} m_q \langle\bar{q}q\rangle - \frac{\delta_{ij} x^2}{192}\langle g_s \bar{q}\sigma\cdot Gq\rangle \\
& + \frac{\mathrm{i}\delta_{ij} x^2 \not{x}}{2^7 \times 3^2} m_q \langle g_s \bar{q}\sigma\cdot Gq\rangle - \frac{t^a_{ij}\sigma_{\alpha\beta}}{192}\langle g_s \bar{q}\sigma\cdot Gq\rangle \\
& + \frac{\mathrm{i} t^a_{ij}}{768}(\sigma_{\alpha\beta}\not{x} + \not{x}\sigma_{\alpha\beta}) m_q \langle g_s \bar{q}\sigma\cdot Gq\rangle \,, \qquad (21)
\end{aligned}
$$

where the vacuum condensates are explicitly exhibited. For a more detailed discussion of the quark propagator, readers are referred to Refs. [32, 33]. The Feynman diagrams corresponding to the various terms in Eq. (20) are schematically illustrated in Fig. 1.

By applying the Borel transformation to Eqs. (18) and (19) and equating the OPE representation with the phenomenological side of the correlation function $\Pi(q^2)$, one can derive the mass of the tetraquark state as

$$
M^k_{J^{PC}}(s_0, M_B^2) = \sqrt{-\frac{L^k_{J^{PC},1}(s_0, M_B^2)}{L^k_{J^{PC},0}(s_0, M_B^2)}} \,, \qquad (22)
$$

$$
\lambda^k_{J^{PC}}(s_0, M_B^2) = \sqrt{\mathrm{Exp}\left(\frac{M^k_{J^{PC}}(s_0, M_B^2)^2}{M_B^2}\right) L^k_{J^{PC},0}(s_0, M_B^2)} \,. \qquad (23)
$$

Here, L_0 and L_1 are respectively defined as

$$
L^k_{J^{PC},0}(s_0, M_B^2) = \int_{s_{\min}}^{s_0} \mathrm{d}s\, \rho^{\mathrm{OPE},k}_{J^{PC}}(s)\mathrm{e}^{-s/M_B^2} + \Pi^{\mathrm{sum},k}_{J^{PC}}(M_B^2) \,, \qquad (24)
$$

and

$$
L^k_{J^{PC},1}(s_0, M_B^2) = \frac{\partial}{\partial\frac{1}{M_B^2}} L^k_{J^{PC},0}(s_0, M_B^2) \,. \qquad (25)
$$

III. NUMERICAL ANALYSIS

In the numerical analysis, we adopt widely accepted input parameters reported in Refs. [34–39], namely $m_u = 2.16^{+0.49}_{-0.26}$ MeV, $m_d = 4.67^{+0.48}_{-0.17}$ MeV, $m_s = (95 \pm 5)$ MeV, $\langle\bar{q}q\rangle = -(0.23 \pm 0.03)^3$ GeV^3, $\langle\bar{s}s\rangle = (0.8 \pm 0.1)\langle\bar{q}q\rangle$, $\langle\bar{q}g_s\sigma\cdot Gq\rangle = m_0^2\langle\bar{q}q\rangle$, $\langle\bar{s}g_s\sigma\cdot Gs\rangle = m_0^2\langle\bar{s}s\rangle$, $\langle g_s^2 G^2\rangle = (0.88 \pm 0.25)$ GeV^4, and $m_0^2 = (0.8 \pm 0.2)$ GeV^2.

Moreover, two additional parameters, s_0 and M_B^2, are introduced in the process of establishing the QCD sum rules. These parameters are determined following the standard procedure by satisfying two well-established criteria [30, 32, 37–39]. The first criterion concerns the convergence of the operator product expansion (OPE), which is ensured by examining the relative contributions of higher-dimensional condensates to the total OPE. A suitable Borel window for M_B^2 is selected such that the OPE remains convergent in the chosen region. The second criterion requires that the pole contribution (PC) from the ground state should dominate over the continuum, typically accounting for more than 50% of the total spectral density [30, 38, 39]. These two criteria can be mathematically expressed as

$$
R^{\mathrm{OPE}} = \left|\frac{L_0^{dim=8}(s_0, M_B^2)}{L_0(s_0, M_B^2)}\right| \,, \qquad (26)
$$

$$
R^{\mathrm{PC}} = \frac{L_0(s_0, M_B^2)}{L_0(\infty, M_B^2)} \,. \qquad (27)
$$

To determine an appropriate value for the continuum threshold s_0, we follow a procedure analogous to that employed in Refs. [32, 37, 39]. In this approach, the goal is to identify an optimal value of s_0 that yields a stable Borel window for the extracted mass of the fully strange tetraquark state. Within this window, the mass prediction should exhibit minimal dependence on the Borel parameter M_B^2, ensuring the reliability of the QCD sum rule analysis. In practical calculations, $\sqrt{s_0}$ is varied by 0.1 GeV around a central value to determine the corresponding

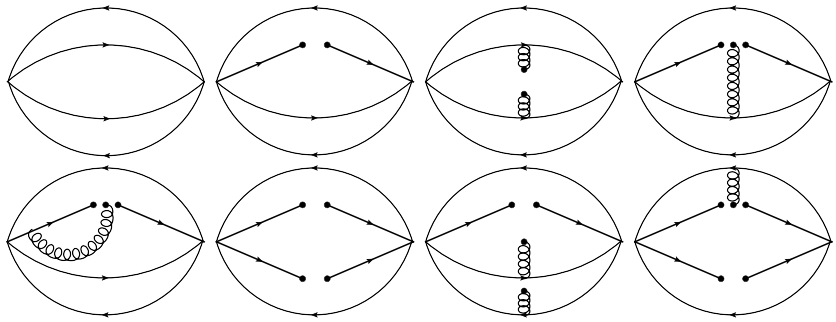

Fig. 1. Typical Feynman diagrams related to the correlation function, where the solid lines denote quarks and spiral ones denote gluons.

lower and upper bounds and, in turn, the uncertainties of $\sqrt{s_0}$ [32].

With the aforementioned preparations, the mass spectrum of the light tetraquark states can now be evaluated numerically. For the current $J^A_{0^{++}}$, as an example, the OPE convergence ratio $R^{\rm OPE}_{A,0^{++}}$ and pole contribution ratio $R^{\rm PC}_{A,0^{++}}$ are plotted as functions of the Borel parameter M_B^2 in Fig. 2(a) for three different values of the continuum threshold $\sqrt{s_0} = 2.8$, 2.9, and 3.0 GeV. The dependence of the extracted mass $M^A_{0^{++}}$ on the Borel parameter is illustrated in Fig. 2(b). From these analyses, an optimal Borel window is identified as $1.4 \le M_B^2 \le 2.2\ {\rm GeV}^2$, within which both the OPE convergence and pole dominance criteria are satisfied. Accordingly, the mass of the fully strange tetraquark state corresponding to the current $J^A_{0^{++}}$ is extracted as

$$M^A_{0^{++}} = (2.23 \pm 0.15)\ {\rm GeV}\,, \tag{28}$$

$$\lambda^A_{0^{++}} = (6.4 \pm 0.6) \times 10^{-3}\ {\rm GeV}^5\,, \tag{29}$$

Using the same analysis framework, we evaluate the masses associated with the other interpolating currents. The corresponding OPE contributions, pole contributions, and extracted mass values are summarized in Table 1. The uncertainties in the mass predictions reported in Table 1 mainly originate from the variations in the input parameters, including the quark masses, vacuum condensates, and continuum threshold parameter $\sqrt{s_0}$.

IV. DISCUSSION ON MASS PREDICTIONS AND DECAY CHANNELS

A. Interpretation of multiple mass predictions

It should be emphasized that the multiple mass values obtained for the 0^{++} channel do not represent theoretical uncertainties of a single state. Rather, they correspond to different interpolating currents with distinct internal structures. Each current may preferentially couple to a particular configuration of the fully strange tetraquark system, leading to different mass predictions and decay patterns.

As an illustrative example, for the 0^{++} states, the structure of the interpolating currents provides insight into their dominant decay channels. Specifically, Eq. (1) corresponds to a coupling of two 0^{-+} components and is therefore more likely to decay into $\eta\eta$; Eq. (2) corresponds to a coupling of two 0^{++} components, favoring the $f_0 f_0$ decay mode; Eq. (3) corresponds to a coupling of two 1^{--} components, with $\phi\phi$ as the dominant decay channel; and Eq. (4) corresponds to a coupling of two 1^{++} components, which preferentially decays into $f_1 f_1$.

It is worth noting that the large mass splittings observed among the predicted 0^{++} states are a natural consequence of the internal structures probed by the different interpolating currents. For instance, $j^B_{0^{++}}$ couples to two 0^{++} mesons, leading to a relatively lower mass, while $j^E_{0^{++}}$ couples to two 2^{--} mesons, resulting in a significantly higher mass. The 2^{--} strange mesons have not yet been observed experimentally, likely due to their high mass. Therefore, the substantial mass difference between $j^B_{0^{++}}$ and $j^E_{0^{++}}$ is physically plausible and reflects the distinct internal structures of the tetraquark states. This point has been explicitly discussed in the revised manuscript to aid interpretation of the mass spectrum.

B. Decay channels of fully-strange tetraquark states

To finally ascertain these fully strange tetraquark states, the straightforward procedure is to reconstruct them from their decay products; however, the detailed characteristics still require further investigation. The decay properties of fully strange tetraquark states strongly depend on their quantum numbers J^{PC}, internal structure, and available phase space. Below, we briefly analyze the dominant and allowed decay channels for each quantum number:

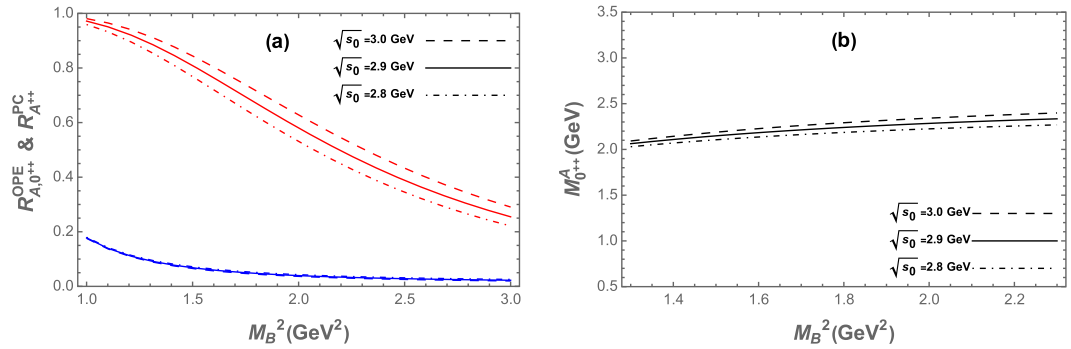

Fig. 2. (color online) (a) Ratios $R^{\rm OPE}_{A,0^{++}}$ and $R^{\rm PC}_{A,0^{++}}$ as functions of the Borel parameter M_B^2 for different values of $\sqrt{s_0}$ for current (1), where blue lines represent $R^{\rm OPE}_{A,0^{++}}$ and red lines denote $R^{\rm PC}_{A,0^{++}}$. (b) Mass of 0^{++} fully strange tetraquark state as a function of the Borel parameter M_B^2 for different values of $\sqrt{s_0}$.

Table 1. Continuum thresholds, Borel parameters, predicted masses, and predicted decay constant of fully strange tetraquark states.

J^{PC}	Current	$\sqrt{s_0}$/GeV	M_B^2/GeV^2	M^X/GeV	λ^X (10^{-3}GeV^5)
0^{++}	A	2.9 ± 0.1	1.4 – 2.2	2.23 ± 0.15	6.4 ± 0.6
	B	2.9 ± 0.1	1.4 – 2.1	2.24 ± 0.16	5.3 ± 0.6
	C	3.1 ± 0.1	1.4 – 2.1	2.50 ± 0.14	11.0 ± 1.2
	D	3.1 ± 0.1	1.4 – 2.1	2.66 ± 0.14	10.8 ± 1.4
	E	3.4 ± 0.1	1.4 – 2.2	3.00 ± 0.08	33.7 ± 5.0
0^{-+}	A	3.3 ± 0.1	1.8 – 2.6	2.57 ± 0.16	7.8 ± 0.3
	B	3.5 ± 0.1	1.6 – 2.4	3.07 ± 0.05	48.9 ± 4.0
0^{--}	A	3.1 ± 0.1	1.4 – 2.1	2.46 ± 0.13	9.4 ± 0.9
1^{--}	A	2.9 ± 0.1	1.4 – 2.1	2.46 ± 0.15	4.7 ± 0.7
	B	3.1 ± 0.1	1.3 – 2.0	2.59 ± 0.09	8.7 ± 1.5
1^{+-}	A	2.9 ± 0.1	1.4 – 2.1	2.29 ± 0.14	3.7 ± 0.3
	B	3.1 ± 0.1	1.3 – 2.0	2.63 ± 0.11	8.2 ± 1.6
1^{++}	A	3.3 ± 0.1	1.5 – 2.2	2.72 ± 0.14	5.3 ± 0.5
	B	3.5 ± 0.1	1.7 – 2.4	3.03 ± 0.08	10.5 ± 0.7

1. For $J^{PC}=0^{++}$ states. The scalar channel can decay via S-wave into two pseudoscalar or two vector mesons. Possible dominant decay modes include $\phi\phi$, $\eta\eta$, $\eta'\eta'$, $\eta\eta'$, f_0f_0, f_1f_1, and $K\bar{K}$ channels. These are all OZI-allowed and likely lead to relatively broad widths, depending on the mass and phase space.

2. For $J^{PC}=0^{-+}$ states. Being a pseudoscalar state, its decays typically proceed via P-wave into $\phi\eta$, $\phi\eta'$, and $K\bar{K}^*$ channels. These modes are sensitive to angular momentum and available energy. If the mass is close to the threshold, the width may be narrow.

3. For $J^{PC}=0^{--}$ states. This is an exotic quantum number not accessible by conventional $q\bar{q}$ mesons. Its decays are constrained and potentially suppressed. Allowed multi-body or radiative decays include $\phi\eta\pi$ and $\eta\eta\gamma$ channels. Due to its exotic nature and limited phase space, this state may be relatively narrow and easier to identify experimentally.

4. For $J^{PC}=1^{--}$ states. This vector state can be directly produced in e^+e^- collisions. Its dominant decays are typically $\phi\eta$, $\phi\eta'$, $K\bar{K}$, and $K^*\bar{K}$ channels.

5. For $J^{PC}=1^{+-}$ states. This axial-vector state can decay via $\phi\eta$, $\phi\eta'$, and $K\bar{K}^*$ channels.

6. For $J^{PC}=1^{++}$ states. Similar to the 1^{+-} case but with different parity, it can decay into $\phi\eta$ and $K^*\bar{K}$ channels. The partial widths and branching ratios are sensitive to internal structure and coupling strengths.

The decay channels of fully strange tetraquarks offer clear experimental signatures, especially through final states such as $\phi\phi$, $\phi\eta$, and $K\bar{K}^*$. Exotic quantum number states like 0^{--} stand out due to their unusual decay modes and suppressed widths, making them key targets for discovery. Future searches at BESIII, Belle II, and LHCb can test these predictions by analyzing invariant mass spectra in strange-rich final states.

The dominant and allowed decay channels of fully-strange tetraquark states are summarized in Table 2.

C. Estimates of relative branching ratios

While a full calculation of decay widths is beyond the scope of the present study, we can provide qualitative estimates of the relative branching ratios of the dominant decay channels using simple phenomenological arguments. These estimates are based on the quantum numbers of the initial states, allowed partial waves, and available phase space.

For the 0^{++} states, the S-wave decays into two pseudoscalar or vector mesons. Among them, decays to channels such as $\phi\phi$ and $\eta\eta$, f_0f_0, and f_1f_1 are expected

Table 2. Dominant and allowed decay channels of fully strange tetraquark states.

J^{PC}	Type	Possible Decay Channels
0^{++}	Scalar	$\phi\phi$, $\eta\eta$, $\eta'\eta'$, $\eta\eta'$, f_0f_0, f_1f_1, $K\bar{K}$
0^{-+}	Pseudoscalar	$\phi\eta$, $\phi\eta'$, $K\bar{K}^*$
0^{--}	Exotic	$\phi\eta\pi$, $\eta\eta\gamma$
1^{--}	Vector	$\phi\eta$, $\phi\eta'$, $K\bar{K}$, $K^*\bar{K}$
1^{+-}	Axial-vector	$\phi\eta$, $\phi\eta'$, $K\bar{K}^*$
1^{++}	Axial-vector	$\phi\eta$, $K^*\bar{K}$

to have relatively large branching ratios due to favorable phase space, CKM suppressed, and OZI-allowed couplings, whereas channels with $K\bar{K}$ may be somewhat suppressed.

For the 0^{-+} states, P-wave decays such as $\phi\eta$, $\phi\eta'$, and $K\bar{K}^*$ are allowed. The $\phi\eta$ channel is likely to dominate due to larger phase space and fewer angular momentum barriers.

For the exotic 0^{--} states, the limited phase space and exotic quantum numbers imply that multi-body decays like $\phi\eta\pi$ and radiative decays such as $\eta\eta\gamma$ may have comparable contributions; however, the total width is expected to be narrow.

For the 1^{--} and 1^{+-} states, vector-pseudoscalar and vector-vector channels such as $\phi\eta$, $\phi\eta'$, $K\bar{K}$, and $K^*\bar{K}$ are favored. Among these, channels with lower mass thresholds and allowed S-wave decays are expected to have relatively higher branching ratios.

For the 1^{++} states, decays into $\phi\eta$ and $K^*\bar{K}$ are expected, with $\phi\eta$ likely being dominant due to phase space considerations.

These qualitative estimates, together with the dominant decay channels summarized in Table 2, provide a more quantitative guidance for experimental searches and help to identify the most promising channels for detecting fully strange tetraquark states.

V. SUMMARY

In this work, we systematically investigated the mass spectrum of fully strange tetraquark states ($ss\bar{s}\bar{s}$) in molecular configurations with quantum numbers $J^{PC} = 0^{++}$, 0^{-+}, 0^{--}, 1^{--}, 1^{+-}, and 1^{++} within the framework of QCD sum rules (QCDSR). By constructing appropriate interpolating currents and applying standard QCDSR techniques, we obtained mass predictions for each quantum number channel. The resulting masses fall within the range of approximately 2.07 to 3.12 GeV, depending on the quantum numbers and interpolating currents used, as summarized in Table 1. Notably, the mass of the $J^{PC} = 1^{+-}$ state shows good agreement with the $X(2300)$ resonance recently reported by the BESIII Collaboration, hinting at a possible exotic tetraquark interpretation. Furthermore, the possible decay modes of these fully strange tetraquark states have been analyzed in detail.

Among these, particular attention is paid to the exotic $J^{PC} = 0^{--}$ channel, which is forbidden in conventional quark-antiquark meson configurations and thus serves as a strong indicator of multiquark or gluonic degrees of freedom. The observation of a state with such quantum numbers would provide compelling evidence for the existence of non-conventional hadrons and offer a direct window into the exotic sector of QCD.

These findings not only enrich the theoretical understanding of multiquark states but also offer concrete and testable predictions for future experimental searches at BESIII, Belle II, LHCb, and other high-energy facilities. Owing to its flavor-pure composition and the absence of mixing with light or heavy quarks, the fully strange tetraquark system provides a particularly clean and ideal environment for probing novel hadronic structures and exploring the nonperturbative dynamics of QCD.

It should be noted that the results in Ref. [72] suggest that the $X(2300)$ prefers an $s\bar{s}q\bar{q}$ structure, whereas the $X(2500)$ and $X(2600)$ are more consistent with an $s\bar{s}s\bar{s}$ configuration. To definitively determine the internal structure of the $X(2300)$, a practical approach is to analyze its various decay products, as discussed in Sec. IV.

To place our mass predictions for fully strange tetraquark states into a broader theoretical context, we compare our results with those obtained in recent quark-model and potential-model studies. For instance, Ref. [22] used a nonrelativistic potential quark model (without invoking a diquark-antidiquark approximation) and predicted an $ss\bar{s}\bar{s}$ tetraquark spectrum with ground and excited 0^{++} masses around 2.2 GeV and up to 3.3 GeV. This mass range overlaps with the lower end of our predicted spectrum; in particular, some of our 0^{++} candidates lie near their ground-state region, providing a nontrivial cross-validation of our sum-rule-based analysis.

More recently, Ref. [28] employed the Gaussian expansion method within a constituent quark potential model to solve the four-body Schrödinger equation and identify resonant states for the $ss\bar{s}\bar{s}$ system. They obtained a series of resonances and compact states in the mass region of 2.7−3.3 GeV, with widths ranging from sub-MeV to approximately 50 MeV. Although their predicted masses are generally higher than our central values, the partial overlap, especially in the excited region, suggests that different modeling assumptions can lead to moderate variations, which is also reflected in our results via different interpolating currents.

The deviations between our sum-rule results and quark-model predictions can be qualitatively understood as arising from fundamentally different assumptions about the internal structure of the tetraquark states (for instance, molecular-type vs compact four-quark configurations), different treatments of interquark interactions and relativistic effects, and methodological limitations inherent to each approach (e.g., truncation of the operator product expansion or basis-set dependence in potential models). As a result, our work should be viewed as complementary to quark-model studies; while these studies capture one class of possible compact/resonant configurations, our sum-rule analysis—especially when employing different interpolating currents—covers a broader set of structural possibilities, including loosely-bound molecular–type states.

In summary, we believe that the consistency (partial overlap) between our predicted mass ranges and those

from potential models lends credence to the plausibility of fully strange tetraquark states and highlights the importance of considering different theoretical frameworks in parallel. This comparison has been added to the revised manuscript to provide a more complete theoretical context for our results.

APPENDIX A: THE RATIOS $R^{\rm OPE}$, $R^{\rm PC}$, AND THE MASSES m ARE PLOPTED AS FUNCTIONS OF BOREL PARAMETER M_B^2

We display the figures for $R^{\rm OPE}$, $R^{\rm PC}$ and the masses m as functions of Borel parameter M_B^2 in Fig. A1−A13.

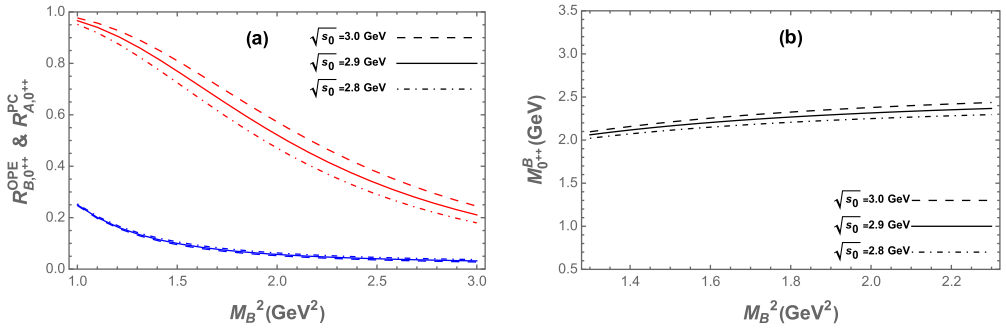

Fig. A1. (color online) (a) Ratios $R^{\rm OPE}_{B,0^{++}}$ and $R^{\rm PC}_{B,0^{++}}$ as functions of the Borel parameter M_B^2 for different values of $\sqrt{s_0}$ for current (2), where blue lines represent $R^{\rm OPE}_{B,0^{++}}$ and red lines denote $R^{\rm PC}_{B,0^{++}}$. (b) Mass of 0^{++} fully strange tetraquark state as a function of the Borel parameter M_B^2 for different values of $\sqrt{s_0}$.

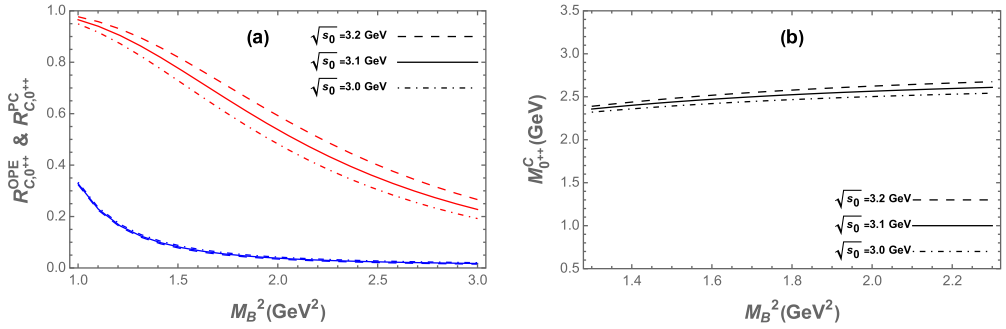

Fig. A2. (color online) (a) Ratios $R^{\rm OPE}_{C,0^{++}}$ and $R^{\rm PC}_{C,0^{++}}$ as functions of the Borel parameter M_B^2 for different values of $\sqrt{s_0}$ for current (3), where blue lines represent $R^{\rm OPE}_{C,0^{++}}$ and red lines denote $R^{\rm PC}_{C,0^{++}}$. (b) Mass of 0^{++} fully strange tetraquark state as a function of the Borel parameter M_B^2 for different values of $\sqrt{s_0}$.

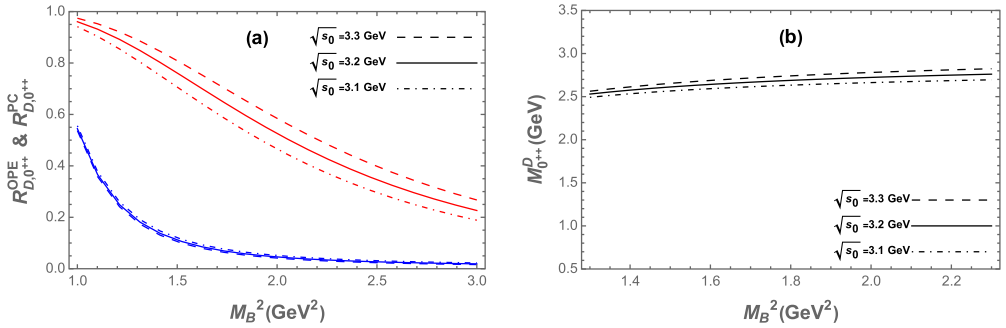

Fig. A3. (color online) (a) Ratios $R^{\rm OPE}_{D,0^{++}}$ and $R^{\rm PC}_{D,0^{++}}$ as functions of the Borel parameter M_B^2 for different values of $\sqrt{s_0}$ for current (4), where blue lines represent $R^{\rm OPE}_{D,0^{++}}$ and red lines denote $R^{\rm PC}_{D,0^{++}}$. (b) Mass of 0^{++} fully strange tetraquark state as a function of the Borel parameter M_B^2 for different values of $\sqrt{s_0}$.

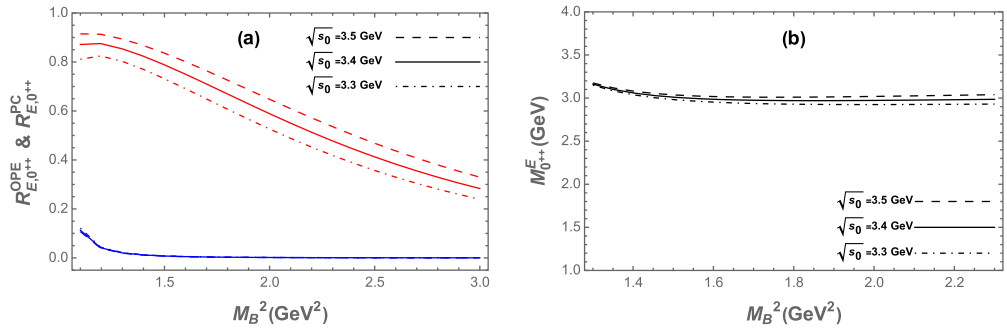

Fig. A4. (color online) (a) Ratios $R^{\rm OPE}_{E,0^{++}}$ and $R^{\rm PC}_{E,0^{++}}$ as functions of the Borel parameter M_B^2 for different values of $\sqrt{s_0}$ for current (5), where blue lines represent $R^{\rm OPE}_{E,0^{++}}$ and red lines denote $R^{\rm PC}_{E,0^{++}}$. (b) Mass of 0^{++} fully strange tetraquark state as a function of the Borel parameter M_B^2 for different values of $\sqrt{s_0}$.

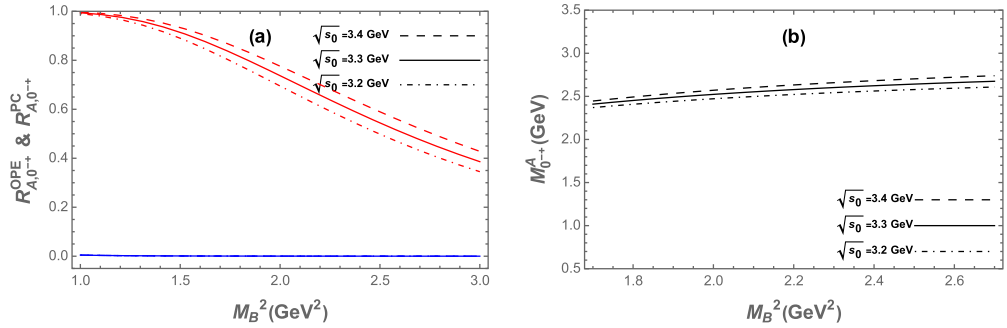

Fig. A5. (color online) (a) Ratios $R^{\rm OPE}_{A,0^{-+}}$ and $R^{\rm PC}_{A,0^{-+}}$ as functions of the Borel parameter M_B^2 for different values of $\sqrt{s_0}$ for current (6), where blue lines represent $R^{\rm OPE}_{A,0^{-+}}$ and red lines denote $R^{\rm PC}_{A,0^{-+}}$. (b) Mass of 0^{-+} fully strange tetraquark state as a function of the Borel parameter M_B^2 for different values of $\sqrt{s_0}$.

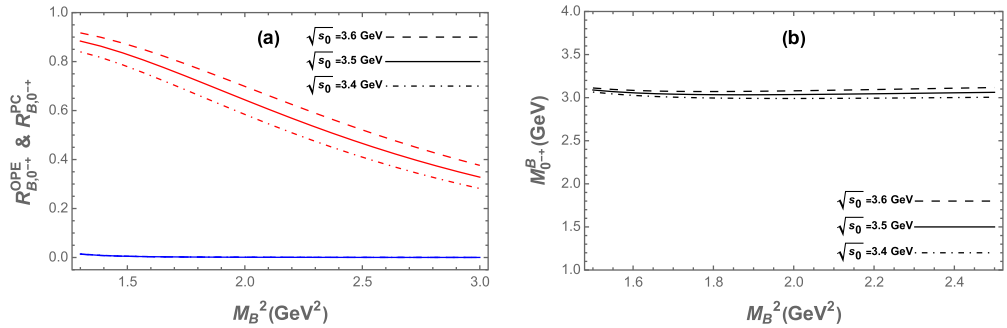

Fig. A6. (color online) (a) Ratios $R^{\rm OPE}_{B,0^{-+}}$ and $R^{\rm PC}_{B,0^{-+}}$ as functions of the Borel parameter M_B^2 for different values of $\sqrt{s_0}$ for current (7), where blue lines represent $R^{\rm OPE}_{B,0^{-+}}$ and red lines denote $R^{\rm PC}_{B,0^{-+}}$. (b) Mass of 0^{-+} fully strange tetraquark state as a function of the Borel parameter M_B^2 for different values of $\sqrt{s_0}$.

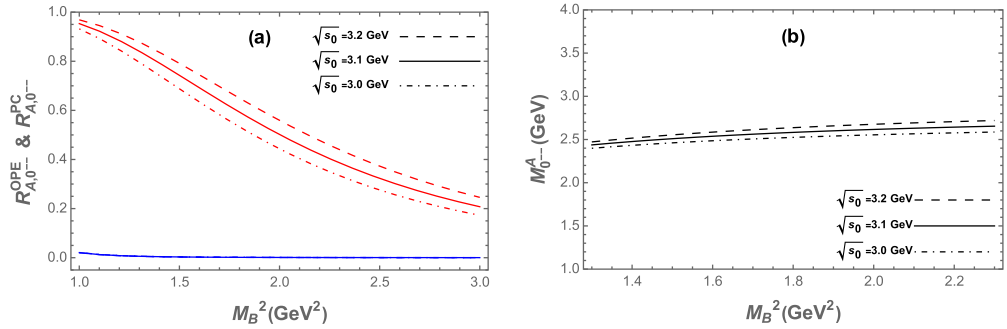

Fig. A7. (color online) (a) Ratios $R^{\rm OPE}_{A,0^{--}}$ and $R^{\rm PC}_{A,0^{--}}$ as functions of the Borel parameter M_B^2 for different values of $\sqrt{s_0}$ for current (8), where blue lines represent $R^{\rm OPE}_{A,0^{--}}$ and red lines denote $R^{\rm PC}_{A,0^{--}}$. (b) Mass of 0^{--} fully strange tetraquark state as a function of the Borel parameter M_B^2 for different values of $\sqrt{s_0}$.

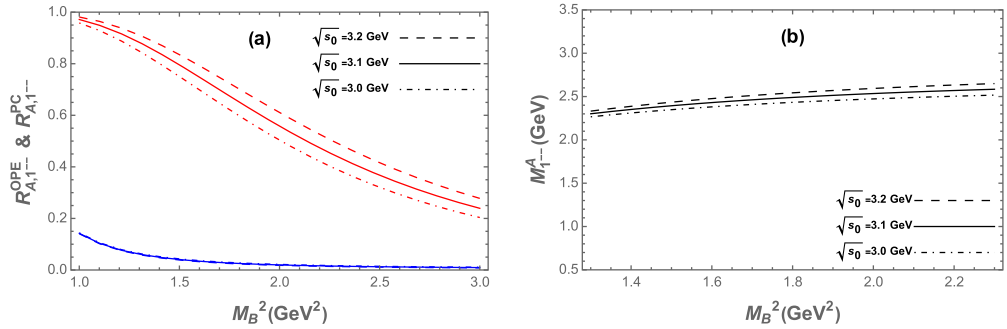

Fig. A8. (color online) (a) Ratios $R^{\rm OPE}_{A,1^{--}}$ and $R^{\rm PC}_{A,1^{--}}$ as functions of the Borel parameter M_B^2 for different values of $\sqrt{s_0}$ for current (9), where blue lines represent $R^{\rm OPE}_{A,1^{--}}$ and red lines denote $R^{\rm PC}_{A,1^{--}}$. (b) Mass of 1^{--} fully strange tetraquark state as a function of the Borel parameter M_B^2 for different values of $\sqrt{s_0}$.

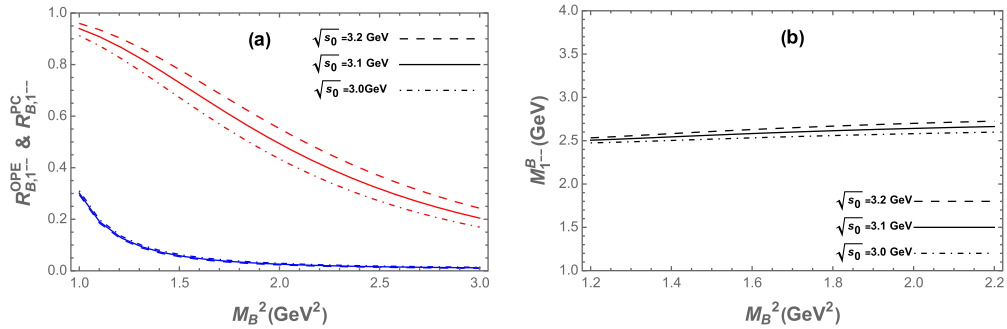

Fig. A9. (color online) (a) Ratios $R^{\rm OPE}_{B,1^{--}}$ and $R^{\rm PC}_{B,1^{--}}$ as functions of the Borel parameter M_B^2 for different values of $\sqrt{s_0}$ for current (10), where blue lines represent $R^{\rm OPE}_{B,1^{--}}$ and red lines denote $R^{\rm PC}_{B,1^{--}}$. (b) Mass of 1^{--} fully strange tetraquark state as a function of the Borel parameter M_B^2 for different values of $\sqrt{s_0}$.

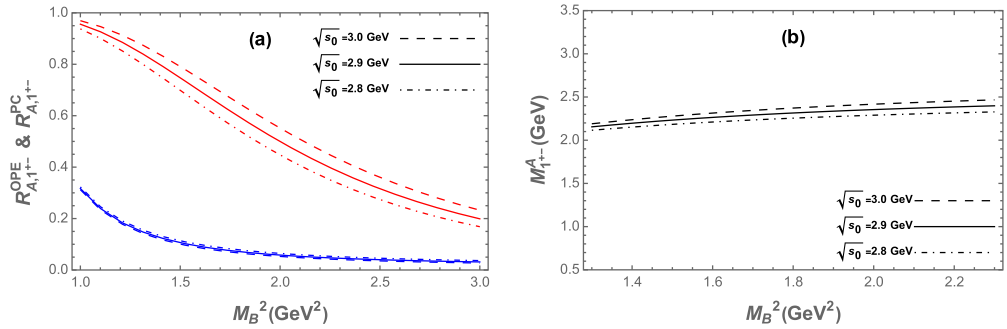

Fig. A10. (color online) (a) Ratios $R^{\rm OPE}_{A,1^{+-}}$ and $R^{\rm PC}_{A,1^{+-}}$ as functions of the Borel parameter M_B^2 for different values of $\sqrt{s_0}$ for current (11), where blue lines represent $R^{\rm OPE}_{A,1^{+-}}$ and red lines denote $R^{\rm PC}_{A,1^{+-}}$. (b) Mass of 1^{+-} fully strange tetraquark state as a function of the Borel parameter M_B^2 for different values of $\sqrt{s_0}$.

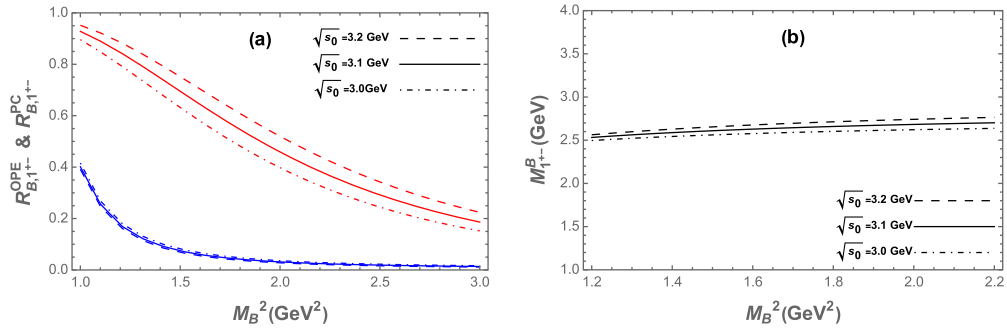

Fig. A11. (color online) (a) Ratios $R^{\rm OPE}_{B,1^{+-}}$ and $R^{\rm PC}_{B,1^{+-}}$ as functions of the Borel parameter M_B^2 for different values of $\sqrt{s_0}$ for current (12), where blue lines represent $R^{\rm OPE}_{B,1^{+-}}$ and red lines denote $R^{\rm PC}_{B,1^{+-}}$. (b) Mass of 1^{+-} fully strange tetraquark state as a function of the Borel parameter M_B^2 for different values of $\sqrt{s_0}$.

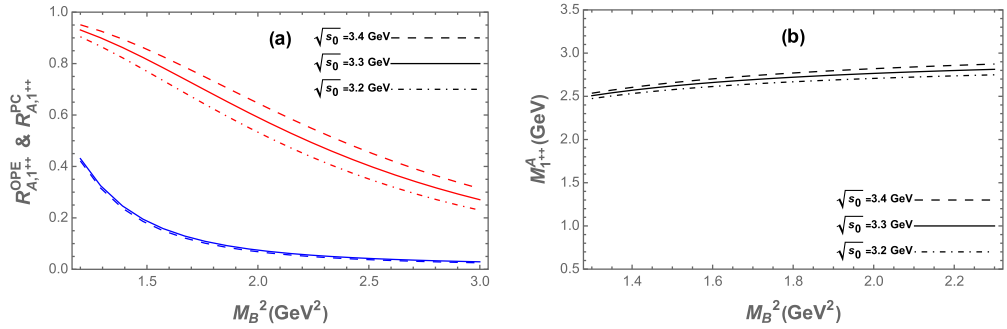

Fig. A12. (color online) (a) Ratios $R^{\rm OPE}_{A,1^{++}}$ and $R^{\rm PC}_{A,1^{++}}$ as functions of the Borel parameter M_B^2 for different values of $\sqrt{s_0}$ for current (13), where blue lines represent $R^{\rm OPE}_{A,1^{++}}$ and red lines denote $R^{\rm PC}_{A,1^{++}}$. (b) Mass of 1^{++} fully strange tetraquark state as a function of the Borel parameter M_B^2 for different values of $\sqrt{s_0}$.

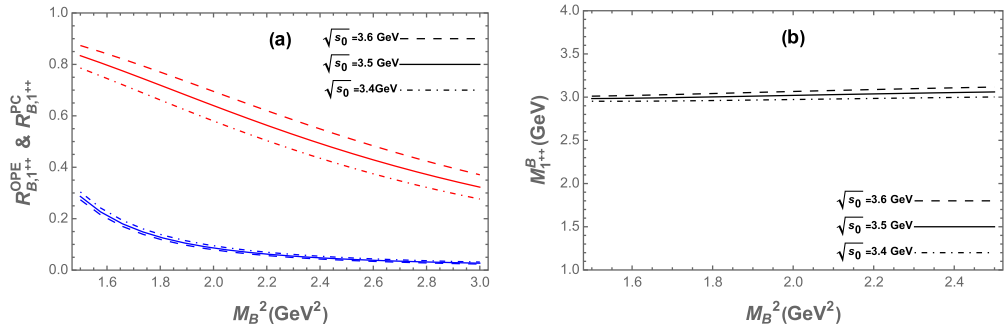

Fig. A13. (color online) (a) Ratios $R^{\rm OPE}_{B,1^{++}}$ and $R^{\rm PC}_{B,1^{++}}$ as functions of the Borel parameter M_B^2 for different values of $\sqrt{s_0}$ for current (14), where blue lines represent $R^{\rm OPE}_{B,1^{++}}$ and red lines denote $R^{\rm PC}_{B,1^{++}}$. (b) Mass of 1^{++} fully strange tetraquark state as a function of the Borel parameter M_B^2 for different values of $\sqrt{s_0}$.

References

[1] M. Gell-Mann, Phys. Lett. **8**, 214 (1964)
[2] G. Zweig, Report No. CERN-TH-401
[3] S. K. Choi *et al*. (Belle Collaboration), Phys. Rev. Lett. **91**, 262001 (2003)
[4] M. Ablikim *et al*. (BESIII Collaboration), Phys. Rev. Lett. **106**, 072002 (2011)
[5] J. Z. Bai *et al*. (BES), Phys. Rev. Lett. **91**, 022001 (2003)
[6] M. Ablikim *et al*. (BESI Collaboration), Phys. Rev. Lett. **95**, 262001 (2005)
[7] M. Ablikim *et al*. (BESIII Collaboration), Chin. Phys. C **34**, 421 (2010)
[8] M. Ablikim *et al*. (BESIII Collaboration), Eur. Phys. J. C **80**, 746 (2020)
[9] M. Ablikim *et al*. (BESIII Collaboration), Phys. Rev. D **93**, 112011 (2016)
[10] M. Ablikim *et al*. (BESIII Collaboration), Phys. Rev. Lett. **124**, 112001 (2020)
[11] M. Ablikim *et al*. (BESIII Collaboration), Phys. Rev. D **95**, 052003 (2017)
[12] M. Ablikim *et al*. (BESIII Collaboration), Phys. Rev. D **97**, 032013 (2018)
[13] M. Ablikim *et al*. (BESIII Collaboration), Phys. Rev. Lett. **124**, 032002 (2020)
[14] M. Ablikim *et al*. (BESIII Collaboration), Phys. Rev. Lett. **134**, 191901 (2025)
[15] Q. Li, L. C. Gui, M. S. Liu *et al*., Chin. Phys. C **45**, 023116 (2021)
[16] L. Y. Xiao, X. Z. Weng, X. H. Zhong *et al*., Chin. Phys. C **43**, 113105 (2019)
[17] S. Ishida and K. Yamada, Phys. Rev. D **35**, 265 (1987)
[18] D. Ebert, R. N. Faustov, and V. O. Galkin, Phys. Rev. D **79**, 114029 (2009)
[19] J. Oudichhya, K. Gandhi, and A. K. Rai, Phys. Rev. D **108**, 014034 (2023)
[20] L. M. Wang, J. Z. Wang, S. Q. Luo *et al*., Phys. Rev. D **101**, 034021 (2020)
[21] K. Chen, C. Q. Pang, X. Liu *et al*., Phys. Rev. D **91**, 074025 (2015)
[22] F. X. Liu, M. S. Liu, X. H. Zhong *et al*., Phys. Rev. D **103**, 016016 (2021)
[23] N. Su and H. X. Chen, Phys. Rev. D **106**, 014023 (2022)
[24] H. Z. Xi, Y. W. Jiang, H. X. Chen *et al*., Phys. Rev. D **108**, 094019 (2023)
[25] V. Patel, J. Oudichhya, and A. K. Rai, Eur. Phys. J. A **61**, 218 (2025)
[26] R. R. Dong, N. Su, and H. X. Chen, Eur. Phys. J. C **82**, 983 (2022)
[27] R. R. Dong, N. Su, H. X. Chen *et al*., Front. in Phys. **11**, 1184103 (2023)
[28] Y. Ma, W. L. Wu, L. Meng *et al*., Phys. Rev. D **110**, 074026 (2024)
[29] Q. Xin and Z. G. Wang, Chin. Phys. C **48**, 033104 (2024)

[30] M. A. Shifman, A. I. Vainshtein, and V. I. Zakharov, Nucl. Phys. B **147**, 385 (1979)
[31] B. D. Wan, S. Q. Zhang, and C. F. Qiao, Phys. Rev. D **106**, 074003 (2022)
[32] R. M. Albuquerque, arXiv: 1306.4671 [hep-ph]
[33] Z. G. Wang and T. Huang, Phys. Rev. D **89**, 054019 (2014)
[34] R. D. Matheus, S. Narison, M. Nielsen *et al*., Phys. Rev. D **75**, 014005 (2007)
[35] C. Y. Cui, Y. L. Liu, and M. Q. Huang, Phys. Rev. D **85**, 074014 (2012)
[36] L. Tang, B. D. Wan, K. Maltman *et al*., Phys. Rev. D **101**, 094032 (2020)
[37] P. Colangelo and A. Khodjamirian, in *At the frontier of particle physics / Handbook of QCD*, edited by M. Shifman (Singapore: World Scientific, 2001)
[38] J. Govaerts, L. J. Reinders, H. R. Rubinstein *et al*., Nucl. Phys. B **258**, 215 (1985)
[39] L. J. Reinders, H. Rubinstein, and S. Yazaki, Phys. Rept. **127**, 1 (1985)
[40] S. Narison, World Sci. Lect. Notes Phys. **26**, 1 (1989)
[41] C. M. Tang, Y. C. Zhao, and L. Tang, Phys. Rev. D **105**, 114004 (2022)
[42] C. F. Qiao and L. Tang, Phys. Rev. Lett. **113**, 221601 (2014)
[43] C. F. Qiao and L. Tang, Eur. Phys. J. C **74**, 2810 (2014)
[44] L. Tang and C. F. Qiao, Nucl. Phys. B **904**, 282 (2016)
[45] C. F. Qiao and L. Tang, EPL **107**, 31001 (2014)
[46] B. D. Wan, L. Tang, and C. F. Qiao, Eur. Phys. J. C **80**, 121 (2020)
[47] C. M. Tang, C. G. Duan, and L. Tang, Eur. Phys. J. C **84**, 743 (2024)
[48] C. F. Qiao and L. Tang, Eur. Phys. J. C **74**, 3122 (2014)
[49] C. M. Tang, C. G. Duan, L. Tang *et al*., Eur. Phys. J. C **85**, 396 (2025)
[50] B. D. Wan and C. F. Qiao, Nucl. Phys. B **968**, 115450 (2021)
[51] B. D. Wan and C. F. Qiao, Phys. Lett. B **817**, 136339 (2021)
[52] S. N. Li and L. Tang, arXiv: 2404.11145 [hep-ph]
[53] B. D. Wan, S. Q. Zhang, and C. F. Qiao, Phys. Rev. D **105**, 014016 (2022)
[54] Y. C. Zhao, C. M. Tang, and L. Tang, Eur. Phys. J. C **83**, 654 (2023)
[55] S. Q. Zhang, B. D. Wan, L. Tang *et al*., Phys. Rev. D **106**, 074010 (2022)
[56] B. D. Wan and C. F. Qiao, arXiv: 2208.14042 [hep-ph]
[57] F. H. Yin, W. Y. Tian, L. Tang *et al*., Eur. Phys. J. C **81**, 818 (2021)
[58] B. D. Wan, Eur. Phys. J. C **84**, 760 (2024)
[59] L. Tang and C. F. Qiao, Eur. Phys. J. C **76**, 558 (2016)
[60] B. C. Yang, L. Tang, and C. F. Qiao, Eur. Phys. J. C **81**, 324 (2021)
[61] B. D. Wan, Nucl. Phys. B **1004**, 116538 (2024)
[62] B. D. Wan and H. T. Xu, Chin. Phys. C **48**, 093103 (2024)
[63] B. D. Wan and Y. R. Wang, Eur. Phys. J. A **60**, 179 (2024)
[64] B. D. Wan and S. Yang, Eur. Phys. J. A **61**, 11 (2025)
[65] W. S. Zhang and L. Tang, arXiv: 2412.11531 [hep-ph]
[66] S. Q. Zhang and C. F. Qiao, Phys. Rev. D **108**, 074017 (2023)
[67] S. Q. Zhang, X. H. Zhang, and C. F. Qiao, JHEP **06**, 122 (2024)
[68] S. Q. Zhang and C. F. Qiao, Phys. Rev. D **110**, 114040 (2024)
[69] X. H. Zhang, S. Q. Zhang, and C. F. Qiao, Eur. Phys. J. C **85**, 693 (2025)
[70] Y. C. Fu, Z. R. Huang, Z. F. Zhang *et al*., Phys. Rev. D **99**, 014025 (2019)
[71] Z. R. Huang, W. Chen, T. G. Steele *et al*., Phys. Rev. D **95**, 076017 (2017)
[72] S. Jafarzade and R. F. Lebed, arXiv: 2505.15704 [hep-ph]